Proc. Fla. State Hort. Soc. 125:67–70. 2012.

Phloem Anatomy of Citrus Trees: Healthy vs. Greening-affected

Ed Etxeberria* and Cody Narciso

University of Florida, IFAS, Citrus Research and Education Center, Lake Alfred, FL 33850

Additional index words. phloem starch, pit fields, sieve elements, sieve pores, symplastic transport

Phloem cells from HLB-affected trees become obstructed with callose and P-protein plugs. The presence of these plugs is believed to hinder the translocation of photoassimilates (nitrogenous and reduced carbon compounds) to the root system. However, even with seemingly collapsed phloem tissue, citrus trees remain viable and produce fruit for some time, suggesting either incomplete plugging of phloem elements or the existence of alternative routes for photoassimilate transport. In this study, we examined the basic structure of phloem tissue from HLB-free and HLB-affected trees under light and scanning electron microscopy. To avoid any possible interference with callose induced by injury during sampling, we employed a freeze substitution technique. Sieve elements from HLB-free trees show sizable lateral pores to phloem and ray parenchyma. Early stage HLB-affected phloem cells contain dark electron dense material and jagged appearing cell walls. Eventually, these cells totally collapse into almost a solid cell-wall barrier. The large number of wall depressions all along the cortex, ray and vascular parenchyma with abundant pit fields, could be an essential anatomical feature necessary to support symplastic transport of photoassimlates in an HLB-compromised phloem system.

Huanglongbing (HLB, or citrus greening) is a highly destructive disease of citrus presumably caused by the fastidious Gram-negative, obligate parasitic, phloem-limited α-protobacterium *Candidatus* Liberibacter ssp. (Bove, 2006; Jagoueix et al., 1994). Of the several species identified worldwide (Kim et al., 2009), *Candidatus* Liberibacter asiaticus (CLas) is the only species found in Florida thus far (Albrecht and Boman, 2009). CLas is vectored by the phloem feeding psyllid *Diaphorina citri* (Halbert and Manjunath, 2004), and transmitted into the phloem stream of citrus leaves during the feeding process.

Phloem cells from HLB-affected trees become obstructed with callose and P-protein plugs (Achor et al., 2010), a common response to wounding or pathogen infection (Evert 1977). These plugs are deposited in both lateral pit fields (Koh et al., 2011) as well as in and around sieve plates (Folimonova and Achor, 2010; Koh et al., 2011). In addition, starch grains are commonly observed within the sieve elements (Folimonova and Achor, 2010). The presence of these plugs and of starch-containing amyloplasts is believed to hinder the transport of photoassimilates (nitrogenous and reduced carbon compounds) from photosynthetic source leaves to the remaining heterotrophic sink tissues. The resulting backlog of reduced carbon compounds in the phloem conduits promotes sugar conversion to starch in virtually all living cells in HLB-affected leaves (Etxeberria et al., 2009), an unmistakable characteristic of HLB-affected trees (Schneider, 1968).

However, two observations place doubts on the soundness of this hypothesis. First, parenchyma cells from woody stems and bark tissue downstream from the leaf canopy also accumulate copious amounts of starch. Second, HLB-affected branches with evident HLB symptoms and seemingly obstructed phloem are capable of producing average fruit for some time (Ikpechukwu et al., 2011). If photassimilate transport were totally blocked at the leaf/petiole level, there would be insufficient carbohydrate to sustain the synthesis of starch in a basipetal direction and to support the growth of developing fruits. Recognizing that phloem plugging and collapse is not localized to one individual HLB-affected sieve tube but is widespread throughout the phloem tissue (Schneider, 1952), we theorize the existence of an ancillary (albeit less efficient) route for photoassimilate transport. To answer this question, we examined the basic structure of phloem tissue from HLB-unaffected and HLB-free leaves under light and scanning electron microscopy. Our observations demonstrate abundant symplastic connections between photosynthetic, vascular and cortex parenchyma cells capable of supporting symplastic transport of photoassimilates.

Materials and Methods

Plant material. Leaves from HLB-affected trees were collected for their visual symptoms from 5-year-old 'Valencia' orange (*Citrus sinensis* L. Osbeck) trees grown at the Citrus Research and Education Center in Lake Alfred, FL. The trees had been previously determined to be HLB-affected by PCR. Control HLB-free samples were obtained from 'Valencia' trees grown in an HLB-free greenhouse.

To avoid any possible interference with callose and P-protein plugs induced by injury during sampling, we employed freeze substitution technique. Leaf petioles were cut off immediately after leaf sampling and frozen in liquid nitrogen. Once in the laboratory, the petioles were transferred to conical centrifuge tubes containing 1.5 mL of cold 100% ethanol. The tubes were placed in the freezer at –20 °C. The ethanol solution was changed every 24 h for 5 d.

Tissue preparation for SEM. Samples were further dehydrated using a Ladd critical point dryer (Ladd Research Industries, Burlington, VT). The dried tissue was then carefully re-cut with a razor blade, mounted on stubs, and coated with gold/palladium using a Ladd sputter coater (Ladd Research Industries). Coated samples were viewed on a Hitachi S530 scanning electron microscope (Tokyo, Japan) and photographed using a Canon EOS Rebel XT digital camera (Tokyo, Japan).

*Corresponding author; phone: (850) 599-3996; email: eetxeber@ufl.edu

Tissue preparation for light microscopy. After alcohol dehydration, samples were fixed in 3% glutaraldehyde in 0.1 M potassium phosphate buffer, pH 7.2, at room temperature for 4 h, and then left overnight in the refrigerator. Afterwards, they were washed in the same buffer and postfixed for 4 h at room temperature in 2% osmium tetroxide in the above buffer. The samples were then dehydrated in an acetone series and embedded in Spurr's resin. For light microscopy, 1-µm sections were cut with glass knives, stained with methylene blue/azure A, and poststained in basic fuchsin. Light micrographs were taken on a Leitz Laborlux S compound microscope (Germany) with a Canon Powershot S31S digital camera (Tokyo, Japan).

Results

HLB-free petiole. Phloem tissue from HLB-free petioles appeared as a ring of compact cells delimited by the distinctively larger xylem vessels to the interior and by thick-walled tracheids to the outside (Figs. 1, 2). The phloem elements have thinner primary walls than all other tissues in the petiole. Large phloem parenchyma cells are invariably observed within the tissue as part of the vascular rays and bordering the inner face of the tracheary ring. Although indistinguishable in light micrographs, sieve plates become evident when viewed at higher magnification under SEM (Fig. 3). The sieve plates were never transversal but always oblique. Sometimes, the plates were arranged at such steep angles that appear as part of the lateral walls as previously reported by Schneider, 1952, and Koh et al., 2012. It is noteworthy that the sizes of individual sieve pores were comparable to or smaller than the diameter of the smallest morphological form expressed by CLas (Bove, 2006; Garnier et al., 1984; Mann et al., 2011; Shokrollah et al., 2010).

Another anatomical characteristic prominent in SEM micrographs were the numerous wall depressions commonplace to all parenchyma cells (Fig. 2). These areas were of approximately 2–5 µm in diameter with distinctly thinner walls than the rest of the cell (Fig. 2). Within the depression, pit fields are abundant, sometimes separated by wall ridges (Fig. 4). Abundant pit fields were also observed in cortex parenchyma (Fig. 5) and epidermal photosyntheic cells (not shown).

HLB-affected petiole. Figure 6 depicts a cross-section of a petiole at an intermediate stage (based on visible symptoms) of HLB development. At this stage, phloem cells appear irregular with jagged boundaries. The darker appearance of the phloem tissue was the result of thickened cell walls (Fig. 6) and from the collapse of the protophloem located at the cortex boundary of the tissue. At this stage, although metaphloem elements are not entirely collapsed, they showed a very dense cytoplasmic content, likely the callose and P-protein plugs associated with HLB (Achor et al., 2010). Starch grains, occasionally seen in healthy leaves (Etxeberria at al., 2009), became prominent in all parenchymatous tissues of the petiole. Although cortex parenchyma appeared to have the

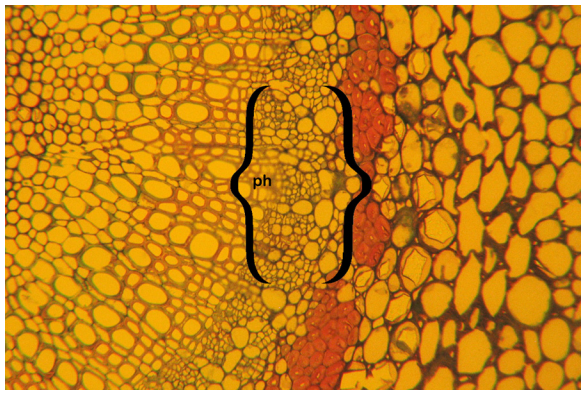

Fig. 1. Cross-section light micrograph of a petiole from a HLB-free tree. Phloem cells (**ph**) have smooth edges and lack starch grains.

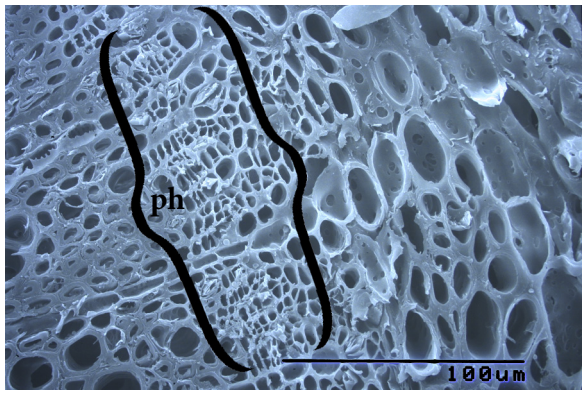

Fig. 2. Scanning electron micrograph of a cross section of a petiole from HLB-free tree. Phloem cells (**ph**) have smooth edges and lack starch grains. Parenchyma rays are evident traversing the vascular tissue and reaching the cortex. The tissue incubated in β-glucanase and α-amylase to remove all interfering polysaccharides.

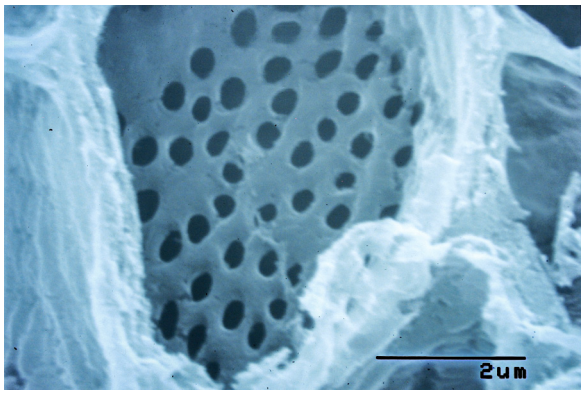

Fig. 3. Scanning electron micrograph of a sieve plate from a petiole mid-rib. The leaf was collected from an HLB-free tree and the tissue incubated in β-glucanase and α-amylase to remove all interfering polysaccharides.

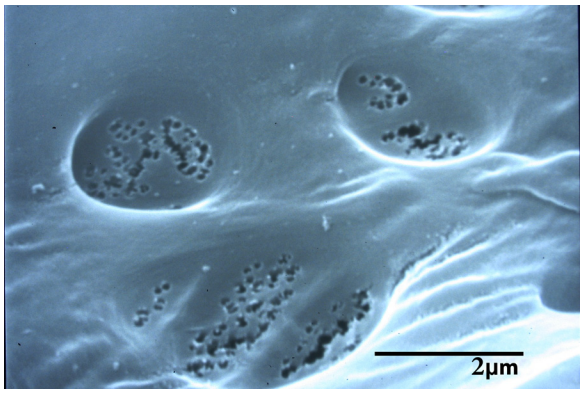

Fig. 4. Scanning electron micrograph of a parenchyma wall depression containing pit fields. The tissue incubated in β-glucanase and α-amylase to remove all interfering polysaccharides.

highest concentration and larger starch grains, xylem, phloem and ray parenchyma also accumulated substantial amounts of starch (Fig. 6). Furthermore, EM micrographs revealed the presence of starch in sieve elements (Folimonova and Achor, 2010). Figure 7 shows the abundance of starch grains in cortical cells. At a more advanced stage of HLB (estimated by visual examination), the entire phloem tissue collapsed, forming an indistinguishable mass of cell wall material (Fig. 8). In very advanced stages, cell crushing extended to the inner areas of cortical cells as shown in Fig. 9. The absence of starch grains in Fig. 9 was due to preliminary incubation of the tissue in β-glucanase and α-amylase to remove all interfering polysaccharides such as callose and starch.

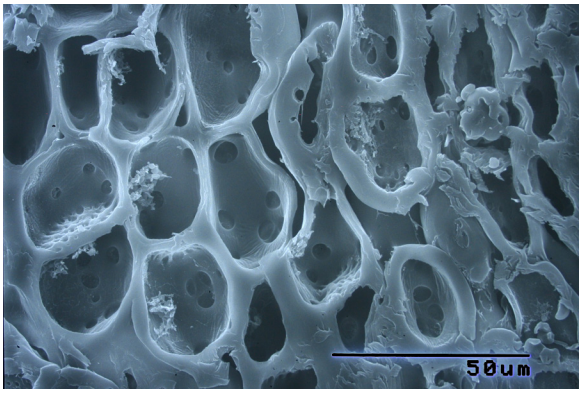

Fig. 5. Scanning electron micrograph of cortex parenchyma showing numerous pit fields. The tissue incubated in β-glucanase and α-amylase to remove all interfering polysaccharides.

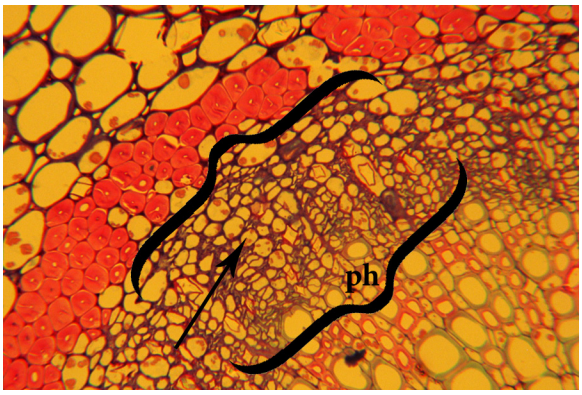

Fig. 6. Cross-section light micrograph of a petiole from a HLB-affected tree. Phloem cells (**ph**) have jagged edges and darker stained cell walls compared to those of Figure 1. Phloem parenchyma cells (**arrowhead**) contain visible starch grains.

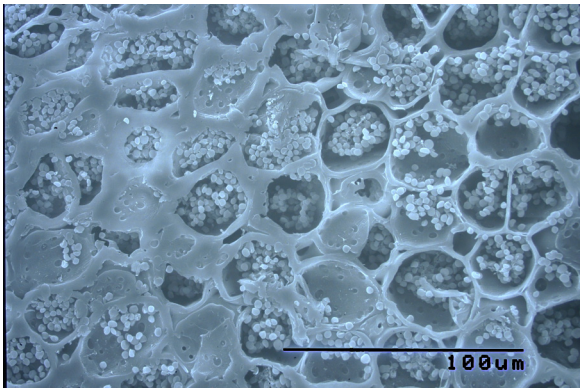

Fig. 7. Scanning electron micrograph of cortex parenchyma from an HLB-affected tree showing copious amount of starch grains and numerous pit fields.

Discussion

When vectored into a citrus leaf by the Asian citrus psyllid *D. citri*, the presumed HLB causing agent CLas unravels a series of physiological and metabolic reactions that culminate in reduced vigor, diminished production, and tree death (Etxeberria et al., 2009). A well-described metabolic change induced by the presence of the bacteria is the deposition of callose plugs throughout the phloem elements, the hyper-accumulation of starch in all aerial parts and its disappearance from the roots (Etxeberria et al., 2009). This preferential sequestration of photoassimilate mostly in the form of starch in leaves and stem parenchyma cells denotes a carbohydrate imbalance that can culminate in tree death.

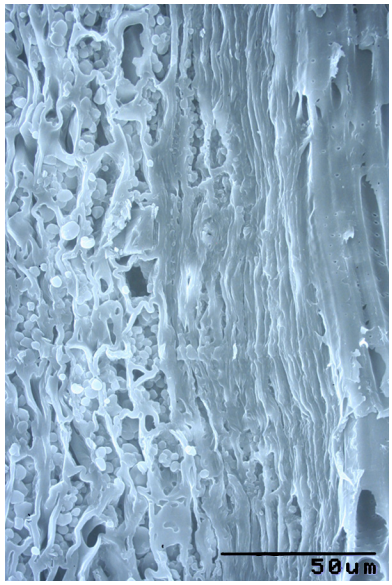

Fig. 8. Radial scanning electron micrograph of an HLB-affected petiole. Phloem cells appear collapsed, forming a solid mass of wall, whereas the cortex parenchyma contain copious amount of starch grains.

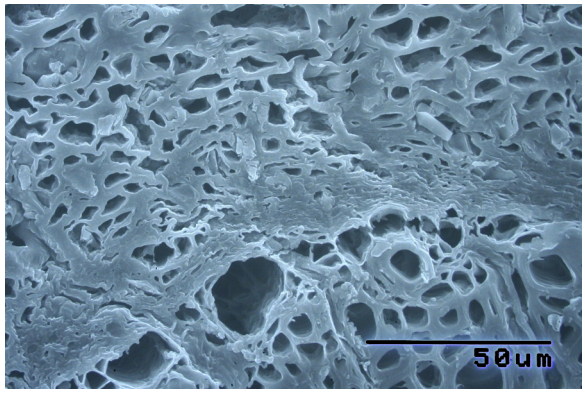

Fig. 9. Cross-section scanning electron micrograph of an HLB-affected petiole at an advanced stage. In this figure, metaphloem tissue has entirely collapsed forming a solid mass of cell wall. The external protophloem and inner part of the cortex are being crushed by the expanding xylem elements.

In his thorough investigation, Schneider (1968) concluded that starch accumulation in HLB-affected leaves results from necrotic phloem pockets formed scattered throughout the vascular system. He proposed that these blockages impeded phloem transport of photoassimilates, creating a backlog of sugars in the leaves, which in turn trigger accelerated rates of starch synthesis. Phloem collapse and blockage has been further detailed by Achor et al. (2010) and Folimonova et al. (2010). Nevertheless, the development of fruit in HLB-affected branches is an indication that photoassimilates are being effectively transported from source leaves despite a severely compromised phloem system. The anatomical analyses presented in this communication support the existence of an alternate non-vascular temporary route of photoassimilates to heterotrophic organs that bypasses the phloem. This conclusion is supported by three observations. First, the complete obliteration of the phloem tissue as the disease advances (Figs. 8, 9) is likely to obstruct all transport through sieve elements. Second, there is the lack of microscopically visible "wound phloem" that characteristically develops along impaired phloem elements (Jacobsen and Eschrich, 1990). Third, the abundant starch reserves in the vascular pith support the effective transport through vascular rays.

Our observations based on static images do not allow us to determine the type of transport route to heterotrophic cells. However, the copious plasmodesmata pit fields (Fig. 4) throughout cortex (Figs. 2, 5) and other parenchyma cells (Fig. 7) revealed the presence of the essential anatomical components necessary to support a symplastic continuum. Whether transport occurs exclusively through a symplastic route or whether it is accompanied by apoplastic movement is a matter that needs further physiological analyses.

The data also raise an intriguing dilemma related to CLas transport through the phloem. From our many images of sieve plates (of which Fig. 3 is a representative sample), and from those of Koh et al. (2012), is evident that the size of sieve pores (<0.5 µm) are highly restrictive to CLas movement. Published studies indicate that CLas exists in two forms (Bove, 2006; Garnier et al. 1984; Mann et al., 2011; Shokrollah et al., 2010): a spherical ~1 µm diameter form and a rod-like form of ~0.25 × 2.5 µm. Disagreements exist, however, based on the difficulties inherent in measuring an organism using thin sections and whether samples came from plant (Bove, 2006; Garnier et al., 1984; Shokrollah et al., 2010) or insect tissue (Mann et al., 2011). Regardless of the source, it is evident that only some individuals within the rod-like population are capable of intracellular movement within the phloem elements.

Literature Cited

Albrecht, U. and K. Bowman. 2009. *Candidatus* Liberibacter asiaticus and Huanglongbing effects on citrus seeds and seedlings. HortScience 44:1967–1973.

Bove, J.M. 2006. Huanglongbing: A destructive, newly-emerging, century-old disease of citrus. J. Plant Pathol. 88:3–37.

Etxeberria, E., P. Gonzalez, D. Achor, and G. Albrigo. 2009. Anatomical distribution of abnormally high levels of starch in HLB-affected Valencia orange trees. Physiol Mol. Plant Pathol. 74:76–83.

Evert, R.F. 1977. Phloem structure and histochemistry. Ann. Rev. Plant Physiol. 28:199–222.

Folimonova, S.Y. and D. Achor. 2010. Early events of citrus greening (Huanglongbing) disease development at the ultrastructural level. Bacteriology 2010:949–958.

Garnier, M., N. Danel, and J.M. Bové. 1984. The greening organism is a Gram negative bacterium, p. 115–124. In: S.M. Garnsey, L.W. Timmer, and J.A. Dodds (eds.). Proc. Ninth Conf. Intl. Org. Citrus Virol. Intl. Org. of Citrus Virologists, University of California, Riverside.

Halbert, S.E. and K.L. Manjunath. 2004. Asian citrus psyllids (Sternorrhyncha: Psyllidae) and greening disease of citrus: A literature review and assessment of risk in Florida. Fla. Entomol. 87:330.

Ikpechukwu, C.O., C.A. Sims, M.D. Danyluk, T.M. Spann, and R.M. Goodrich. 2011. Effect of fruit size and huanglongbing disease on orange juice attributes. Proc. Fla. State. Hort. Soc. 124:202–206.

Jacobsen, K.R. and W. Eschrich. 1990. Translocation of photoassimilates in wound-sieve tubes. Planta 181:335–342.

Jagoueix, S., J.M. Bove, and M. Garnier. 1994. The phloem-limited bacterium of greening disease of the proteobacteria is a member of the alpha subdivision of the *Proteobacteria*. Intl. J Syst. Bacteriol. 44:379–386.

Kim, J.S., U.S. Sagaram, J.K. Burns, J.L. Li, and N. Wang. 2009. Response of sweet orange (*Citrus sinensis*) to '*Candidatus* Liberibacter asiaticus' infection: Microscopy and microarray analyses. Phytopathology 99:50–57.

Koh, E-J., L. Zhou, D.S. Wiliams, J. Park, N. Ding, Y-P. Duan, and B-H. Kang. 2012. Callose deposition in the phloem plasmodesmata and inhibition of phloem transport in citrus leaves infected with "*Candidiatus Liberibacter asiaticus*". Protoplasma 249:687–697.

Mann, R.S., K. Pelz-Ttelinski, S.L. Herman, S. Tiwari, and L. Stelinski. 2011. Sexual transmission of a plant pathogenic bacterium, *Candidiatus* Liberibacter asiaticus, between conspecific insect vectors during mating. PLoS One 6:e29197

Schneider, H. 1968. Anatomy of greening-disease sweet orange shots. Phytopathology 58:1155–1160.

Schneider, H. 1952. The phloem of sweet orange tree trunk and the seasonal production of xylem and phloem. Hilgardia 12:331–365.

Shokrollah, H., T.L. Abdullah, K. Sijam, and S.N.A. Abdullah. 2010. Ultrastructures of *Candidiatus* Liberibacter asiaticus and its damage in huanglongbing (HLB) infected citrus. African J. Biotechnol. 9:5897–5901.